

## EFFECT OF THE VISCOSITY PROPERTIES OF ICE ON THE DEFLECTION OF AN ICE SHEET SUBJECTED TO A MOVING LOAD

V. M. Kozin<sup>1</sup> and A. V. Pogorelova<sup>2</sup>

UDC 532.59:539.3:534.1

*Steady-state rectilinear motion of a load on an ice sheet modeled by a viscoelastic plate is considered. The viscoelastic properties of ice are described using the linear Maxwell and Kelvin–Voigt models and a generalized Maxwell–Kelvin model. Calculated vertical displacements and strains of the ice plate are compared with available experimental data.*

**Key words:** *incompressible liquid, viscoelastic plate, steady-state motion of load, ice sheet.*

1. The hydrodynamic problem of a load moving on a continuous ice is modeled by a system of surface pressures which moves above a floating ice plate [1, 2].

We consider an infinite region covered with continuous ice on which a given system of surface pressures  $q$  moves at a velocity  $u$ . The coordinate system attached to the load is arranged as follows: the plane  $xOy$  coincides with the ice–water unperturbed interface, the  $x$  direction coincides with the direction of motion of the load, and the  $z$  axis is directed vertically upward. It is assumed that water is an ideal incompressible liquid of density  $\rho_2$  and the motion of the liquid is potential. The ice sheet is modeled by a viscoelastic homogeneous isotropic plate which is initially not stressed. The linear viscoelastic material simulating ice is described using the Maxwell and Kelvin–Voigt models and a generalized Maxwell–Kelvin model [3]. In the case of pure shear, the behavior of a Maxwell body can be described by a mechanical model consisting of a spring and a viscous damper connected in series, and the behavior of a Kelvin–Voigt body by a model consisting of a spring and a viscous damper connected in parallel. In the case of a one-dimensional state, the generalized Maxwell–Kelvin model considered in the present paper represents Maxwell and Kelvin units connected in series. This model takes into account instantaneous elastic response, viscous flow and delayed elastic response.

By analogy with [1, 4], using the generalized model of a viscoelastic Maxwell–Kelvin material to describe the deformation of an ice sheet under the action of a moving load, it is possible to derive the following equation of small oscillations of a floating viscoelastic plate:

$$\begin{aligned} & \frac{G_M h^3}{3} \left( -u \frac{\partial}{\partial x} + \tau_K u^2 \frac{\partial^2}{\partial x^2} \right) \nabla^4 w + \left[ \tau_M^{-1} + \left( 1 + \frac{G_M}{G_K} + \frac{\tau_K}{\tau_M} \right) \left( -u \frac{\partial}{\partial x} \right) + \tau_K u^2 \frac{\partial^2}{\partial x^2} \right] \\ & \times \left( q + \rho_2 g w + \rho_1 h u^2 \frac{\partial^2 w}{\partial x^2} - \rho_2 u \left( \frac{\partial \Phi}{\partial x} \right) \Big|_{z=0} \right) = 0. \end{aligned} \quad (1.1)$$

Here  $G_M = E_M/[2(1+\nu)]$  and  $G_K = E_K/[2(1+\nu)]$  are the shear elastic moduli of ice corresponding to Maxwell and Kelvin materials,  $E_M$  and  $E_K$  are Young moduli for Maxwell and Kelvin bodies, respectively,  $\nu$  is the Poisson ratio,  $\tau_M$  and  $\tau_K$  are stress and strain relaxation times of ice, respectively,  $h(x, y)$  is the ice thickness,  $\rho_1(x, y)$  is the ice density,  $w(x, y)$  vertical displacement of ice, and  $\Phi = \Phi(x, y, z)$  is a function of the liquid velocity potential which satisfies the Laplace equation  $\Delta \Phi = 0$ . Below, it is assumed that  $\rho_1$  and  $h$  are constants. As the calculated

<sup>1</sup>Komsomol'sk-on-Amur State Technical University, Komsomol'sk-on-Amur 681013. <sup>2</sup>Institute of Machine Science and Metallurgy, Far East Division, Russian Academy of Sciences, Komsomol'sk-on-Amur 681005; sasha@imim.ru. Translated from Prikladnaya Mekhanika i Tekhnicheskaya Fizika, Vol. 50, No. 3, pp. 147–157, May–June, 2009. Original article submitted January 14, 2008; revision submitted March, 24, 2008.

values of the shear modulus  $G$  and ice density  $\rho_1$  it is necessary to adopt their normalized values determined as integral quantities over the plate thickness.

Under the assumption that ice deforms as a Maxwell linear viscoelastic material, Eq. (1.1) becomes

$$\frac{G_M h^3}{3} \left( -u \frac{\partial}{\partial x} \right) \nabla^4 w = \left( \frac{1}{\tau_M} - u \frac{\partial}{\partial x} \right) \left( -q - \rho_2 g w - \rho_1 h u^2 \frac{\partial^2 w}{\partial x^2} + \rho_2 u \left( \frac{\partial \Phi}{\partial x} \right) \Big|_{z=0} \right). \quad (1.2)$$

In case of a linearly elastic material with a lay (Kelvin–Voigt material), the equation of small oscillations of a plate is written as [1, 4, 5]

$$\frac{G_K h^3}{3} \left( 1 - u \tau_K \frac{\partial}{\partial x} \right) \nabla^4 w + \rho_1 h u^2 \frac{\partial^2 w}{\partial x^2} + \rho_2 g w - \rho_2 u \left( \frac{\partial \Phi}{\partial x} \right) \Big|_{z=0} = -q. \quad (1.3)$$

The boundary condition on the bottom of the reservoir is

$$\frac{\partial \Phi}{\partial z} \Big|_{z=-H} = 0 \quad (1.4)$$

( $H = H_1 - b$ , where  $H_1$  is the reservoir depth and  $b = \rho_1 h / \rho_2$  is the depth of ice immersion in static equilibrium). For greater depths, where  $H_1$  is much greater than  $h$ , it can be assumed that  $H \approx H_1$ .

On the ice–water interface, the following linearized kinematic condition is imposed

$$\frac{\partial \Phi}{\partial z} \Big|_{z=0} = -u \frac{\partial w}{\partial x}. \quad (1.5)$$

It is assumed that in the given moving coordinate system, the pressure  $q$  does not depend on time, i.e.,  $q = q(x, y)$ . The system of moving pressures is described by a function  $q(x, y)$  in the form [5, 6]

$$\begin{aligned} q(x, y) &= (q_0/4)[\tanh(\alpha_1(x + L/2)) - \tanh(\alpha_1(x - L/2))] \\ &\times [\tanh(\alpha_2(y + L/(2\omega))) - \tanh(\alpha_2(y - L/(2\omega)))], \end{aligned} \quad (1.6)$$

where  $q_0$  is the nominal pressure,  $\omega = L/B$ ,  $L$  and  $B$  are the length and width of the rectangular area to which the load is applied, and  $\alpha_1$  and  $\alpha_2$  are parameters that characterize the deviation of the pressure distribution in the longitudinal and transverse directions from a rectangular shape. The larger the values of  $\alpha_1$  and  $\alpha_2$ , the closer the pressure distribution shape to a rectangular shape. For  $\alpha_1 \rightarrow \infty$  and  $\alpha_2 \rightarrow \infty$ , the pressure  $q$  is equivalent to the pressure  $q_0$  which is uniformly distributed over the rectangle.

**2.** In the construction of the analytical solution of the problem, it is assumed that the functions  $w(x, y)$ ,  $\Phi(x, y, z)$ , and  $q(x, y)$  can be represented in the form of a decomposition into Fourier integrals in the variables  $x$  and  $y$ :

$$\begin{aligned} \Phi(x, y, z) &= \frac{1}{4\pi^2} \int_0^\infty k dk \int_{-\pi}^\pi d\theta \iint_{\Omega} (F_1 \exp(-kz) + F_2 \exp(kz)) \\ &\times \exp[ik((x - x_1) \cos \theta + (y - y_1) \sin \theta)] dx_1 dy_1, \\ q(x, y) &= \frac{1}{4\pi^2} \int_0^\infty k dk \int_{-\pi}^\pi d\theta \iint_{\Omega} q(x_1, y_1) \exp[ik((x - x_1) \cos \theta + (y - y_1) \sin \theta)] dx_1 dy_1, \\ w(x, y) &= \frac{1}{4\pi^2} \int_0^\infty k dk \int_{-\pi}^\pi d\theta \iint_{\Omega} w(x_1, y_1) \exp[ik((x - x_1) \cos \theta + (y - y_1) \sin \theta)] dx_1 dy_1. \end{aligned} \quad (2.1)$$

Here  $\Omega$  is the region of distribution of the load  $q$  [in the case of a load of the form (1.6), the region  $\Omega$  is the entire plane  $x_1 O y_1$ ];  $F_1$  and  $F_2$  are unknown functions of the variables  $x_1$ ,  $y_1$ ,  $k$ , and  $\theta$ . Substituting expressions (2.1) into the boundary condition (1.1) with the use of the boundary condition (1.4) and the kinematic condition (1.5) and making the change of variables  $\lambda = k$ ,  $\alpha = k \cos \theta$  and simple transformations, we obtain the following formula for calculating the deflection of the ice plate simulated by a Maxwell–Kelvin material subjected to a steadily moving load of the form (1.6):

$$\begin{aligned} \operatorname{Re}(w(x, y)) = & \frac{q_0}{\rho_2 u^2 \alpha_1 \alpha_2} \int_0^\infty \lambda^2 \tanh(\lambda H) \int_0^\lambda \frac{\sin(\alpha L/2) \sin(\sqrt{\lambda^2 - \alpha^2} L/(2\omega))}{\sinh(\pi\alpha/(2\alpha_1)) \sinh(\pi\sqrt{\lambda^2 - \alpha^2}/(2\alpha_2))} \\ & \times \frac{\cos(\sqrt{\lambda^2 - \alpha^2} y)}{\sqrt{\lambda^2 - \alpha^2} (\xi^2 + \eta^2)} \left[ \left( (1 - \tau_M \tau_K u^2 \alpha^2) \cos(\alpha x) + \tau_M u \alpha \left( 1 + \frac{G_M}{G_K} + \frac{\tau_K}{\tau_M} \right) \sin(\alpha x) \right) \xi \right. \\ & \left. + \left( (1 - \tau_M \tau_K u^2 \alpha^2) \sin(\alpha x) - \tau_M u \alpha \left( 1 + \frac{G_M}{G_K} + \frac{\tau_K}{\tau_M} \right) \cos(\alpha x) \right) \eta \right] d\alpha d\lambda, \end{aligned} \quad (2.2)$$

where

$$\begin{aligned} \xi &= \frac{G_M h^3 \lambda^5 \tau_M \tanh(\lambda H)}{3\rho_2} \tau_K \alpha^2 + (1 - \tau_M \tau_K u^2 \alpha^2) \left( -\frac{g\lambda \tanh(\lambda H)}{u^2} + \frac{\rho_1 h \alpha^2 \lambda \tanh(\lambda H)}{\rho_2} + \alpha^2 \right), \\ \eta &= \frac{G_M h^3 \lambda^5 \tau_M \tanh(\lambda H)}{3\rho_2 u} \alpha - \left( 1 + \frac{G_M}{G_K} + \frac{\tau_K}{\tau_M} \right) \tau_M u \alpha \left( -\frac{g\lambda \tanh(\lambda H)}{u^2} + \frac{\rho_1 h \alpha^2 \lambda \tanh(\lambda H)}{\rho_2} + \alpha^2 \right). \end{aligned}$$

To obtain a formula for the deflection of the ice plate simulated by a Maxwell material under the action of the moving load, it is possible to perform similar calculations for Eq. (1.2) using the Fourier transform or to eliminate the Kelvin unit from the solution obtained for the generalized model (2.2), i.e., set  $\tau_K = 0$  and  $G_K = \infty$ . The formula for the vertical displacement of the ice plate using the Maxwell model is written as

$$\begin{aligned} \operatorname{Re}(w(x, y)) = & \frac{q_0}{\rho_2 u^2 \alpha_1 \alpha_2} \int_0^\infty \lambda^2 \tanh(\lambda H) \int_0^\lambda \frac{\sin(\alpha L/2) \sin(\sqrt{\lambda^2 - \alpha^2} L/(2\omega))}{\sinh(\pi\alpha/(2\alpha_1)) \sinh(\pi\sqrt{\lambda^2 - \alpha^2}/(2\alpha_2))} \\ & \times \cos(\sqrt{\lambda^2 - \alpha^2} y) \frac{(\cos(\alpha x) + \tau_M u \alpha \sin(\alpha x)) \xi + (\sin(\alpha x) - \tau_M u \alpha \cos(\alpha x)) \eta}{\sqrt{\lambda^2 - \alpha^2} (\xi^2 + \eta^2)} d\alpha d\lambda, \end{aligned} \quad (2.3)$$

where

$$\begin{aligned} \xi &= -\frac{g\lambda \tanh(\lambda H)}{u^2} + \frac{\rho_1 h \alpha^2 \lambda \tanh(\lambda H)}{\rho_2} + \alpha^2, \\ \eta &= \frac{G_M h^3 \lambda^5 \tau_M \tanh(\lambda H)}{3\rho_2 u} \alpha - \tau_M u \alpha \left( -\frac{g\lambda \tanh(\lambda H)}{u^2} + \frac{\rho_1 h \alpha^2 \lambda \tanh(\lambda H)}{\rho_2} + \alpha^2 \right). \end{aligned}$$

The expression for the deflection of the plate simulated by a Kelvin–Voigt material is obtained similarly from Eq. (1.3) using the Fourier transform (2.1) and conditions (1.4) and (1.5). If the pressure is described by function (1.6), this expression becomes

$$\begin{aligned} \operatorname{Re}(w(x, y)) = & \frac{q_0}{\rho_2 u^2 \alpha_1 \alpha_2} \int_0^\infty \lambda^2 \tanh(\lambda H) \int_0^\lambda \frac{\sin(\alpha L/2) \sin(\sqrt{\lambda^2 - \alpha^2} L/(2\omega))}{\sinh(\pi\alpha/(2\alpha_1)) \sinh(\pi\sqrt{\lambda^2 - \alpha^2}/(2\alpha_2))} \\ & \times \cos(\sqrt{\lambda^2 - \alpha^2} y) \frac{\cos(\alpha x) \xi + \sin(\alpha x) \eta}{\sqrt{\lambda^2 - \alpha^2} (\xi^2 + \eta^2)} d\alpha d\lambda, \end{aligned} \quad (2.4)$$

where

$$\begin{aligned} \xi &= -\frac{G_K h^3 \lambda^5 \tanh(\lambda H)}{3\rho_2 u^2} - \frac{g\lambda \tanh(\lambda H)}{u^2} + \frac{\rho_1 h \alpha^2 \lambda \tanh(\lambda H)}{\rho_2} + \alpha^2, \\ \eta &= \frac{G_K h^3 \lambda^5 \tau_K \tanh(\lambda H)}{3\rho_2 u} \alpha. \end{aligned}$$

**3.** To determine the boundaries of the region of applicability of the Maxwell and Kelvin–Voigt models and the generalized Maxwell–Kelvin model, it is necessary to compare the results of calculations by formulas (2.2)–(2.4) and available experimental data [2, 7, 8]. Takizava [7] gives the results of the tests performed at lake Sharoma in Hokkaido (Japan) on February 4–10, 1981. In particular, the experimental data used for comparison with theoretical

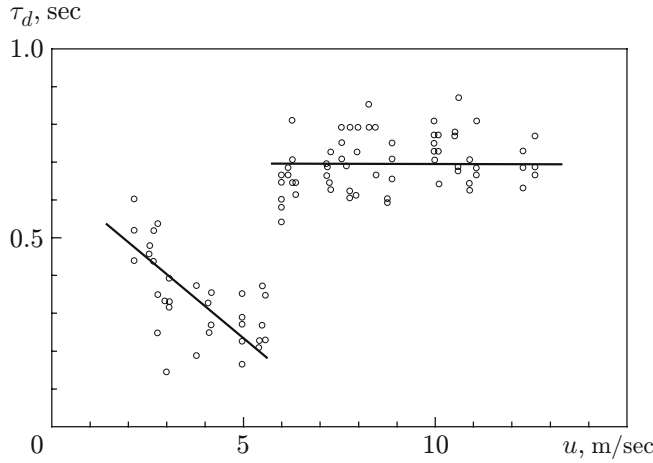


Fig. 1. Delay time (relative to the center of the load) and the maximum plate deflection versus velocity [2, 7]: the points are experimental data, and the curves are approximation results.

results include a time dependence of the vertical displacement of an ice sheet at a distance of 1 m from the line of motion of a snowmobile at various velocities. Squire et al. [8] (and a later paper (fuller version) [2]) give the results of the Project Kiwi 131 experiment (performed near Tent island in McMurdo sound), in particular, readings of strain gauges located at 30 and 100 m from the line of motion of a cargo pickup.

The results of calculations by formulas (2.2)–(2.4) are compared with experimental data [7] for the following values of the main characteristics of load, ice, and reservoir taken from [7]:  $\rho_1 = 900 \text{ kg/m}^3$ ,  $\rho_2 = 1000 \text{ kg/m}^3$ ,  $\nu = 1/3$ ,  $\alpha_1 L = \alpha_2 L = 10$ ,  $\omega = 2.56$ ,  $y = 1 \text{ m}$ ,  $h = 0.075 \text{ m}$ ,  $H = 6.8 \text{ m}$ ,  $L = 1.23 \text{ m}$ ,  $B = 0.48 \text{ m}$ , and  $q_0 = 406.5 \text{ Pa}$ .

The relaxation times  $\tau_M$  and  $\tau_K$  are determined using the dependences of the delay time  $\tau_d$  of the maximum deflection of the ice sheet (relative to the center of the load) on velocity obtained in experiments [7] (Fig. 1). In [2, 7], the delay time is associated with the relaxation time  $\tau$  for the viscoelastic model of an ice sheet. The dependences shown in Fig. 1 by straight line segments can be approximately represented as

$$\tau = \begin{cases} 0.69(1 - u/\sqrt{gH}), & u < u_{\min}, \\ 0.69, & u \geq u_{\min}, \end{cases} \quad (3.1)$$

where  $u_{\min} = 2(Dg^3/(27\rho_2))^{1/8}$  is the minimum phase velocity of propagation of flexural-gravity waves [1, 2];  $D = Eh^3/(12(1 - \nu^2))$ .

In Fig. 2, curves 1 and 2 are the vertical displacements of the ice plate modeled by Maxwell material (2.3) and Kelvin–Voigt material (2.4), respectively, for the parameter values indicated above for the relaxation times  $\tau_M$  and  $\tau_K$  given by formulas (3.1) and for  $E_M = E_K = 5 \cdot 10^9 \text{ Pa}$ . Dotted curves 3 show experimental data [2, 7]. From the results of comparison of curves 1–3 in Fig. 2, it follows that at low velocities of motion ( $u < u_{\min}$ ), the Kelvin–Voigt model describes the maximum deflections more accurately than the Maxwell model. At subcritical velocities, the Maxwell model gives overestimated (to 150%) values of the maximum deflections. However, at higher velocities ( $u \geq u_{\min}$ ), the Maxwell model provides more accurate maximum values of the deflection amplitude; in addition, this model describes wave precursors. The Kelvin–Voigt model (curve 2 in Fig. 2) at higher velocities ( $u \geq u_{\min}$ ) does not describe wave precursors, and the maximum deflections obtained using this model is only 60–80% of experimental values.

Based on the results of calculations using the Maxwell and Kelvin–Voigt models and taking into account that the relaxation times  $\tau_M$  and  $\tau_K$  have different physical meanings, as the basic dependence for the strain relaxation time  $\tau_K$  we choose the dependence corresponding to the inclined straight line in Fig. 1, and as the stress relaxation time  $\tau_M$ , we use the dependence corresponding to the horizontal straight line in Fig. 1. It is assumed that, in the generalized Maxwell–Kelvin model, the relaxation times  $\tau_M$  and  $\tau_K$  are given by the formulas

$$\tau_M = \begin{cases} 0.69\sqrt{gH}/u, & u < \sqrt{gH}, \\ 0.69, & u \geq \sqrt{gH}, \end{cases} \quad \tau_K = \begin{cases} 0.69(1 - u/\sqrt{gH}), & u < u_{\min}, \\ 0, & u \geq u_{\min}. \end{cases} \quad (3.2)$$

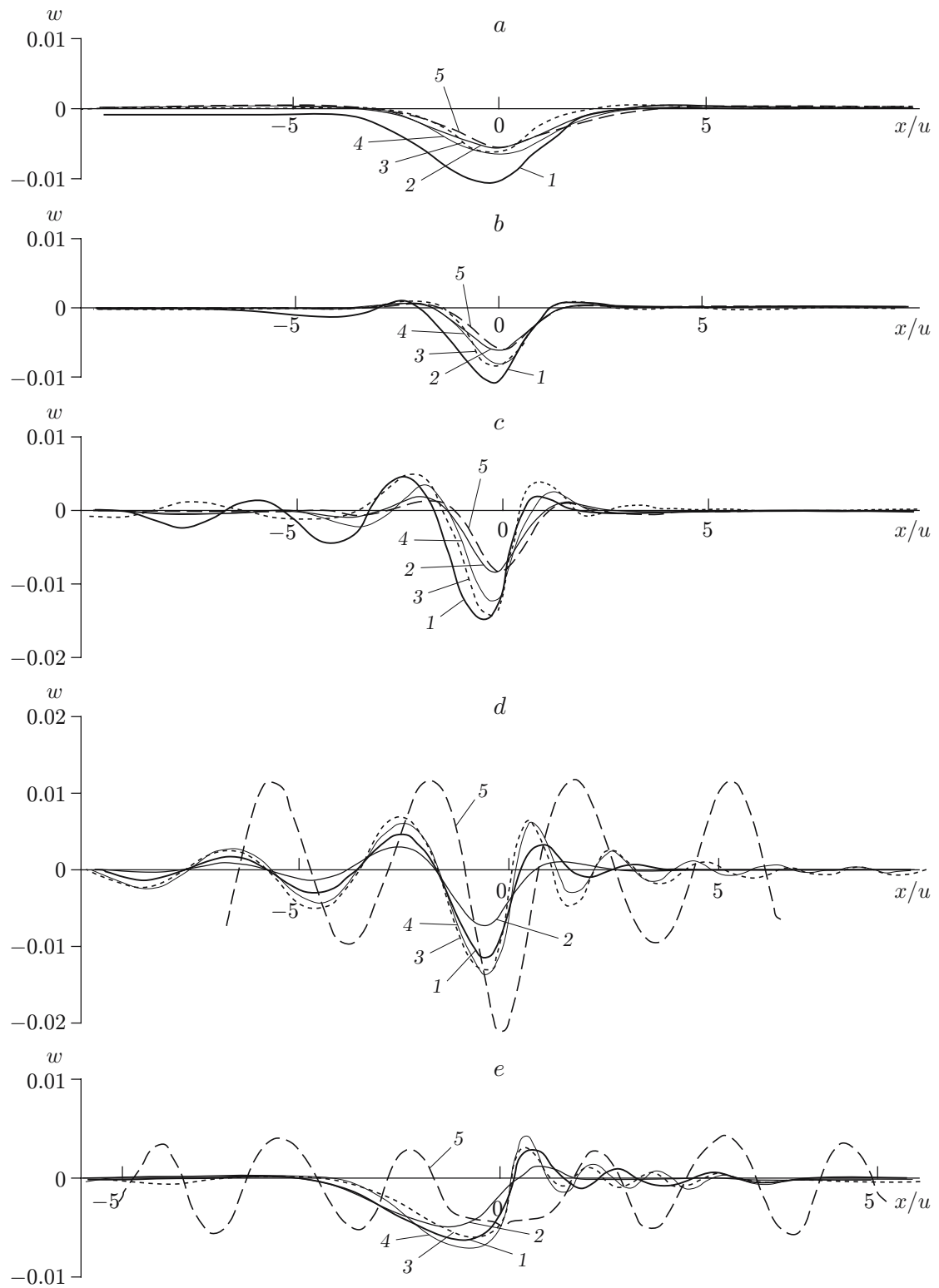


Fig. 2. Vertical displacement of the ice plate modeled by various viscoelastic materials subjected to a steadily moving load for  $u = 2.2$  (a),  $4.2$  (b),  $5.5$  (c),  $6.2$  (d), and  $8.9$  m/sec (e); 1) Maxwell material; 2) Kelvin-Voigt material; 3) experimental data [2, 7]; 4) generalized Maxwell-Kelvin material; 5) absolutely elastic material.

An analysis of the mechanical model of the Maxwell unit suggests that the stress relaxation time  $\tau_M$  and the shear elastic modulus of ice  $G_M$  are interrelated: if the stress relaxation time  $\tau_M$  increases with decreasing velocity on the interval  $u < \sqrt{gH}$ , the elastic modulus  $G_M$  increases as  $u \rightarrow 0$ . Thus, as  $u \rightarrow 0$ , the Maxwell unit degenerates and the generalized model tends to the Kelvin–Voigt model. It can be assumed that the elastic moduli of ice  $E_M$  and  $E_K$  are given by the formulas

$$E_M = \begin{cases} E_0\sqrt{gH}/u, & u < \sqrt{gH}, \\ E_0, & u \geq \sqrt{gH}, \end{cases} \quad E_K = E_0, \quad (3.3)$$

where  $E_0 = 5 \cdot 10^9$  Pa is the Young modulus of an isotropic homogeneous elastic ice plate under experimental conditions [7]. We note that, in the region  $u \geq u_{\min}$ , the vanishing of the relaxation time  $\tau_K$  leads to the formation of several humps of the flexural wave propagating ahead of the load.

Curves 4 in Fig. 2 shows calculated vertical displacements of the ice plate simulated by the generalized Maxwell–Kelvin model using formulas (2.2), (3.2), and (3.3) for the parameter values indicated above. From an analysis of curves 1–4 in Fig. 2, it follows that the generalized model fairly accurately describes experimental data [7] over the entire interval of the velocities considered. The maximum deflections obtained for this model differ from experimental values by not more than 10%. The model describes the behavior of the flexural wave ahead of the load and the gravity wave behind it in the case of critical and supercritical velocities. At low (subcritical) velocities of motion, the generalized Maxwell–Kelvin model coincides with the Kelvin–Voigt model, and at higher (supercritical) velocities, it differs insignificantly from the Maxwell model. Thus, the Kelvin–Voigt model (2.4) is preferred at low (subcritical) velocities and the Maxwell model (2.3) at the critical and supercritical velocities taking into account the elementary dependence of the relaxation time on velocity (3.1) for Young modulus  $E_0 = 5 \cdot 10^9$  Pa for both models.

Assuming that, in the generalized model (2.2), the relaxation times are equal ( $\tau_K = \tau_M$ ) and are given by formula (3.1), the calculation results will be in quantitative agreement with experimental data [7]. However, at low velocities of motion ( $u = 2.2$  and  $4.2$  m/sec), the deflection amplitude will exceed in magnitude the experimental values by 30–40%, and at near-critical and supercritical velocities ( $u = 6.2$  and  $8.9$  m/sec), the maximum deflections will coincide with those obtained in experiments but the wave precursors will have only two theoretical humps instead of 4–6 experimental humps.

Curves 5 in Fig. 2 correspond to calculations of the vertical displacement of an elastic ice plate (ignoring viscosity forces) subjected to a moving load at various velocities. This result can be obtained by setting  $\tau_M = \infty$  in the Maxwell model [in formula (2.3)] or by setting  $\tau_K = 0$  in the Kelvin–Voigt model [in formula (2.4)]. Curves 5 are obtained for the parameter values indicated above and  $E = 5 \cdot 10^9$  Pa. It is evident that, at subcritical velocities ( $u = 2.2, 4.2$ , and  $5.5$  m/sec), the deflection of the ice plate has the shape of a symmetric cup, which corresponds to the Kelvin–Voigt solution. At supercritical velocities of motion within the framework of the employed integral method of solution, the linear model of an elastic plate subjected to a moving load gives undamped flexural-gravity waves; calculations of the deflection  $w$  for large values of the coordinate  $x$  yield divergent improper integrals.

Figure 3 shows the deflections of the ice sheet calculated by formulas (2.2), (3.2), and (3.3) for the parameter values indicated above. The damping of flexural-gravity waves with distance from the site of application of the load is shown. This effect is observed in experiments [7] but is absent in numerical solutions [9, 10]. Thus, accounting for the viscosity for the ice plate even in a linear formulation provides a fairly accurate description of experimental data. In addition, from Fig. 3 follows that behind the load in the ice plate, a small concavity in the form of a trench along the direction of motion of the load is formed, in addition to the flexural-gravity wave. This effect is not observed in the solution of the problem of motion of a load on an elastic plate or on a viscoelastic plate simulated by a Kelvin–Voigt body. This suggests that it is the introduction of the Maxwell unit, which is responsible for viscous flow of the loaded material, leads to the occurrence of creep deformation of the ice plate. From an analysis of Fig. 3 and curves 1 in Fig. 2, it follows that the creep strain (viscous deflection of the plate under the load and behind it along the trajectory of motion) increases with decreasing velocity of motion and decreases with distance from the site of application of the load. The formation of a small trench-shaped concavity of the ice plate behind the load is confirmed in a theoretical paper [11], in which Fig. 12 shows the wave profile in a direction perpendicular to the motion at a distance 100 m from the site of application of the load.

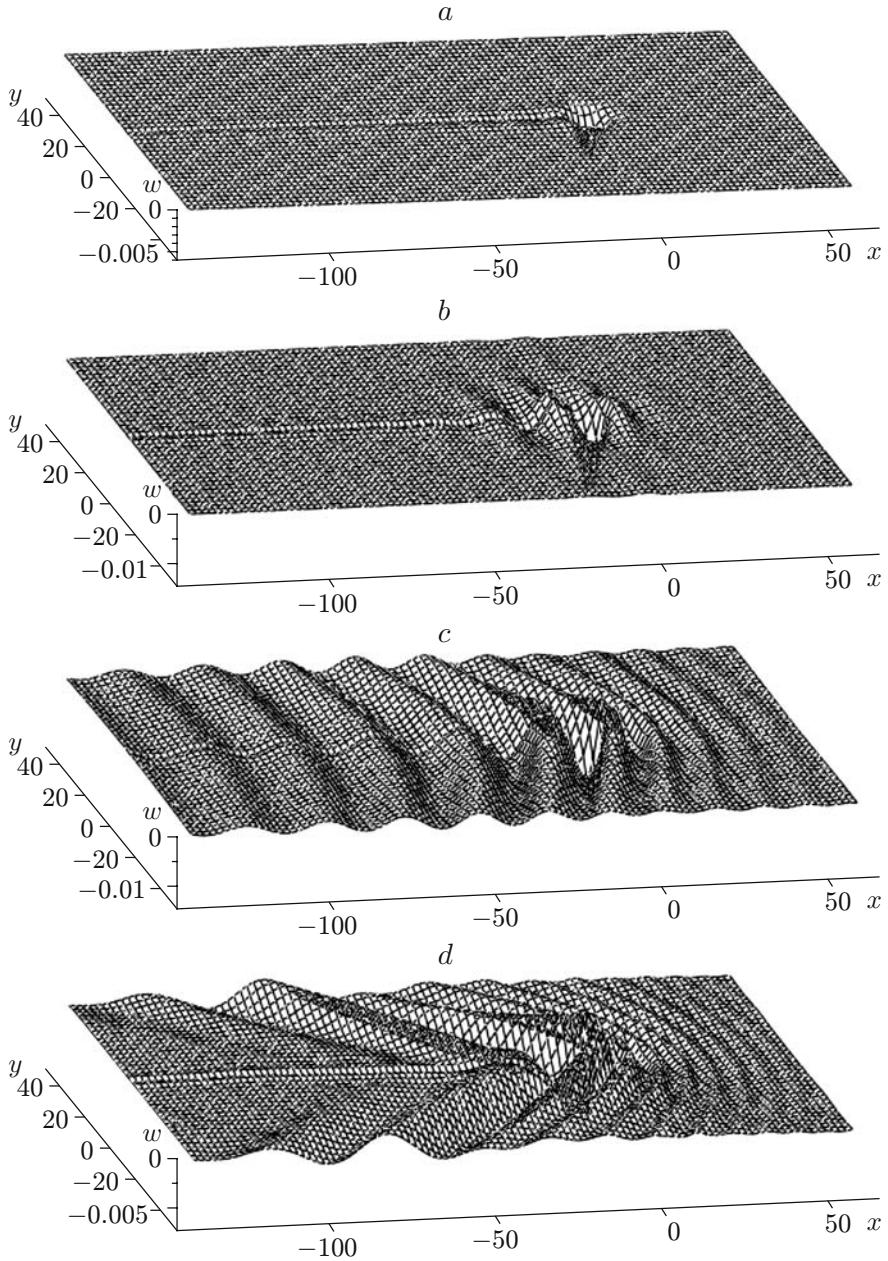


Fig. 3. Deflection of the ice sheet at various velocities of steady-state motion of the load for  $u = 2.2$  (a),  $5.5$  (b),  $6.2$  (c), and  $8.9$  m/sec (d).

For a comparison with experimental results [2, 8], the strain was calculated by the formula

$$\varepsilon_{11} = -\frac{h}{2} \frac{\partial^2 w}{\partial x^2}$$

using formulas (2.2), (3.2), and (3.3).

In Fig. 4, the solid curves show the strains of the ice surface along the line parallel to the midline of motion of the load and located at a distance 30 m from it for the following parameter values:  $\rho_1 = 900 \text{ kg/m}^3$ ,  $\rho_2 = 1000 \text{ kg/m}^3$ ,  $\nu = 1/3$ ,  $\alpha_1 L = \alpha_2 L = 10$ ,  $L = 2.5 \text{ m}$ ,  $h = 1.6 \text{ m}$ ,  $H = 400 \text{ m}$ ,  $\omega = 2$ ,  $q_0 = 6586 \text{ Pa}$ ,  $y = 30 \text{ m}$ ,  $D = 1.536 \cdot 10^9 \text{ N} \cdot \text{m}$ , and  $E_0 = 4 \cdot 10^9 \text{ Pa}$ . It should be noted that the dimensions of the load ( $L$  and  $\omega$ ) approximately correspond to the

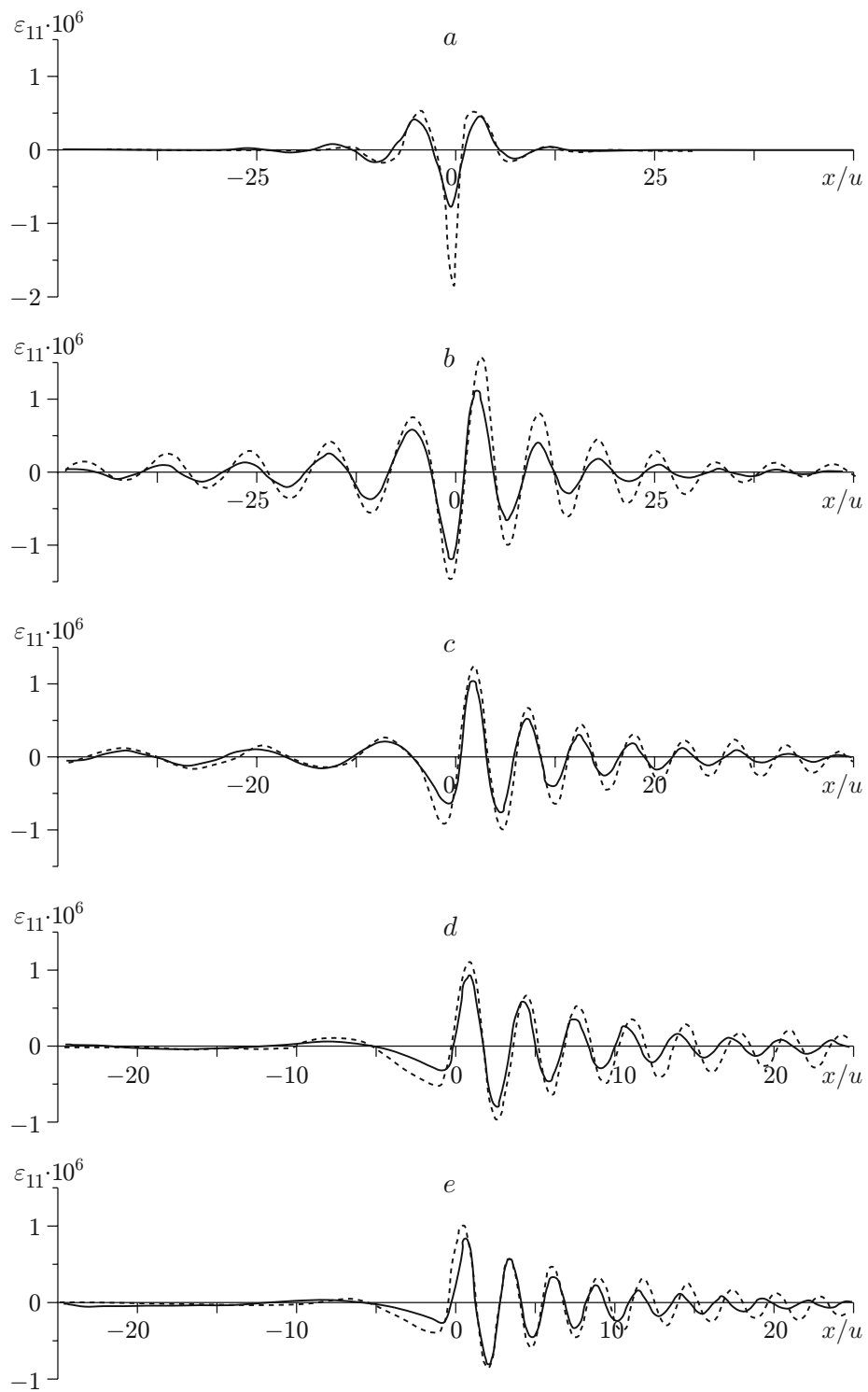


Fig. 4. Strain of the viscoelastic ice plate for  $u = 17.5$  (a), 18.4 (b), 20.7 (c), 25.8 (d), and 28.5 m/sec (e); the solid and dotted curves correspond to calculation results and experimental data, respectively.

dimensions of the distributed pressure produced by the cargo pickup; the value of  $q_0$  corresponds to the mass of the load (pickup) of 2100 kg [2, 8]. For the data used in experiments [2, 8],  $\sqrt{gH} = 62.6$  km/sec and  $u_{\min} = 18$  km/sec. The dashed curves in Fig. 4 correspond to experimental data [2, 8] representing the readings of a strain gauge located at a distance of 30 m from the line of motion of the cargo pickup.

From Fig. 4 it follows that results of calculations using the generalized Maxwell–Kelvin model are in good qualitative agreement with the data of the Project Kiwi 131 experiment [2, 8]. The quantitative difference between the theoretical and experimental results can be explained by the fact that the calculations used approximate dimensions of the load (pickup). It should be noted that the plate strains calculated using the generalized Maxwell–Kelvin model are in good qualitative agreement with the results of calculations [2] using an asymptotic formula valid for a limited range of load velocities at large distances from the site application of the load.

**4.** The results of the study lead to the following conclusions. The results of calculations using the Maxwell, Kelvin–Voigt, and Maxwell–Kelvin linear models of a viscoelastic material are in good agreement with the results of known experiments. The dependence of the relaxation time on velocity is described by formula (3.1) for the simple Maxwell or Kelvin–Voigt models or the more complex formula (3.2) for the generalized Maxwell–Kelvin model. The generalized Maxwell–Kelvin model fairly accurately describes the maximum deflections of the viscoelastic plate, the gravity wave behind the load, and the flexural wave ahead of the load.

The deflections under a moving load at subcritical velocities predicted by the model of an elastic plate are similar to those obtained using the Kelvin–Voigt model. These results are the more similar to the experimental data the higher the velocity of motion of the load. With the framework of the integral method of solution for  $u \geq u_{\min}$ , the model of an absolutely elastic plate gives undamped flexural-gravity waves.

It should be noted that formulas (3.1) and (3.2) correspond to the motion of a load on deep water ( $u_{\min} < \sqrt{gH}$ ). In the case of motion of a load on shallow water ( $\sqrt{gH} < u_{\min}$ ), to avoid negative relaxation times in formulas (3.1) and (3.2) in the interval  $u \in (\sqrt{gH}; u_{\min})$ , it is proposed to interchange the quantities  $u_{\min}$  and  $\sqrt{gH}$  in these formulas. This assumption, however, also needs to be verified.

This work was supported by the program Development of the Scientific Potential of the Higher School (2006–2008) (Grant No. RNP.2.1.2.1809).

## REFERENCES

1. D. E. Khesin, *Dynamics of an Ice Sheet* [in Russian], Gidrometeoizdat, Leningrad (1967).
2. V. A. Squire, R. J. Hosking, A. D. Kerr, and P. J. Langhorne, *Moving Loads on Ice Plates*, Kluwer Acad. Publ., Dordrecht (1996).
3. G. E. Mase, *Theory and Problems of Continuum Mechanics*, McGraw-Hill, New York (1970).
4. A. M. Freudenthal and H. Geiringer, “The mathematical theory of the inelastic continuum,” in: *Encyclopedia of Physics*, Springer-Verlag, Berlin (1958).
5. V. M. Kozin and A. V. Pogorelova, “Wave resistance of an air-cushion vehicle in unsteady motion over an ice sheet,” *J. Appl. Mech. Tech. Phys.*, **44**, No. 2, 71–79 (2003).
6. L. J. Doctors and S. D. Sharma, “The wave resistance of an aircushion vehicle in steady and acceleration motion,” *J. Ship Res.*, **16**, No. 4, 248–260 (1972).
7. T. Takizava, “Deflection of a floating sea ice sheet induced by a moving load,” *Cold Regions Sci. Technol.*, **11**, 171–180 (1985).
8. V. A. Squire, W. H. Robinson, P. J. Langhorne, and T. G. Haskell, “Vehicles and aircraft on floating ice,” *Nature*, **333**, 159–161 (1988).
9. F. Milinazzo, M. Shinbrot, and N. W. Evans, “A mathematical analysis of the steady response of floating ice to the uniform motion of rectangular load,” *J. Fluid Mech.*, **287**, 173–197 (1995).
10. R. W. Yeung and J. W. Kim, “Structural drag and deformation of a moving load on a floating plate,” in: *Proc. of the 2nd Int. Conf. on Hydroelasticity in Marine Technology* (Fukuoka, Jpn., Dec. 1–3, 1998), Yomei Printing Cooperative Soc., Fukuoka (1998), pp. 77–88.
11. K. Wang, R. J. Hosking, and F. Milinazzo, “Time-dependent response of a floating viscoelastic plate to an impulsively started moving load,” *J. Fluid Mech.*, **521**, 295–317 (2004).